2021 8th International Conference on Power and Energy Systems Engineering (CPESE 2021), 10–12 September 2021, Fukuoka, Japan

Robust DC microgrid operation with power routing capabilities

James Amankwah Adu[a],[*], Futoshi Furuta[b], Tohru Kohno[b]

[a] *Department of Electrical, Electronic and Information Engineering, University of Bologna, Bologna, Italy*
[b] *Research and Development Group, Hitachi, Ltd., 1-280, Kokubunji-shi, Tokyo 185-8601, Japan*

Abstract

This paper proposes a robust DC microgrid (MG) operation scheme for intentional power routing (PR) within the MG or between the MG and the utility grid (UG). The MG consists of a photovoltaic (PV) system, a battery energy storage system (BESS), and AC loads connected to the UG via a DC/AC power conditioning system. The operation is achieved by controlling the UG converter and the converter of the BESS in the slack mode with the same or different terminal voltages. In this way, the bus voltage is regulated in a variable range while the magnitude and direction of power exchange between the UG and the MG are realized at the primary voltage control level. The procedure to select the voltage references of the terminals and the control schemes are presented. The system has been implemented in PSIM environment and simulation results proves the reliability and stability of the design.

1. Introduction

Due to the superior advantages such as higher efficiency, lower costs, no frequency or reactive power regulation issues and better compliance with consumer electronics over its AC counterpart, the DC MG concept has attracted significant research interest (e.g. [1,2]). In a DC MG, power balance is manifested only by the DC bus voltage thus to guarantee a stable operation, there should be an effective control of the DC bus voltage.

The present state of the art for MG power flow management consists of the master–slave, droop control schemes and their variants [2]. In the master–slave control scheme, a single converter acts as the slack unit (master) to regulate the system bus voltage while the other converters (slaves) operate in the current controlled mode [3]. In the droop control scheme, multiple slack units regulate the bus voltage to a common reference value by ensuring power balance between energy sources, storage devices and loads in the system [4–6]. A higher secondary control level is usually employed to restore the voltage deviations produced by the droop control [7]. In either of the control

---

* Corresponding author.
 E-mail address: jamesamankwah.adu@gmail.com (J.A. Adu).

schemes, power flow within the MG or between the MG and the UG takes place only when there is variation in DC voltage due to power imbalance between generation and demand.

The DC MG operation proposed in this paper is a modified form of the droop control and incorporates intentional PR capabilities, i.e., intentional energy transaction between the MG and the UG considering the effect of real-time electricity purchase and sale price. This is achieved by operating each terminal at different voltage level. In a typical DC MG configuration consisting of distributed generations (DG) such as wind or PV, energy storage, loads and connection to the UG, the proposed scheme is realized while maximizing energy extraction from the DGs in the following manner: DG terminals are operated in maximum power point tracking MPPT mode (when there is connection to the UG or energy storage units) or operated in the MG bus voltage control (BVC) mode (in the islanded mode with no energy storage units); energy export terminals are kept at higher voltage respect to bus voltage; energy import terminals are kept at lower voltage respect to bus voltage. This paper presents the BVC, PR strategy and the control techniques of the various terminals needed to implement the proposed scheme.

2. Structure, operation modes and power routing strategy of DC microgrid system

2.1. System configuration

The system consists of a PV system, BESS and AC loads. The system is connected to the UG via a voltage source converter (VSC) as shown in Fig. 1. The MG bus voltage is regulated in the range 360–400 V by the presence of a slack terminals in the system. Depending on the operation mode of the system, the UG, BESS or PV system may operate in the slack mode. A MG module consisting of a computer and a power router element is coupled to the network via a LAN connection. The power router module and its software installed on the computer supports the management and power exchange between the MG and the UG. The power router can detect the demand of power from the UG or sale of power to the UG and communicate that information to the power router software module. A detailed development of the computer and power routing configuration is not presented. Also, protection schemes are not designed.
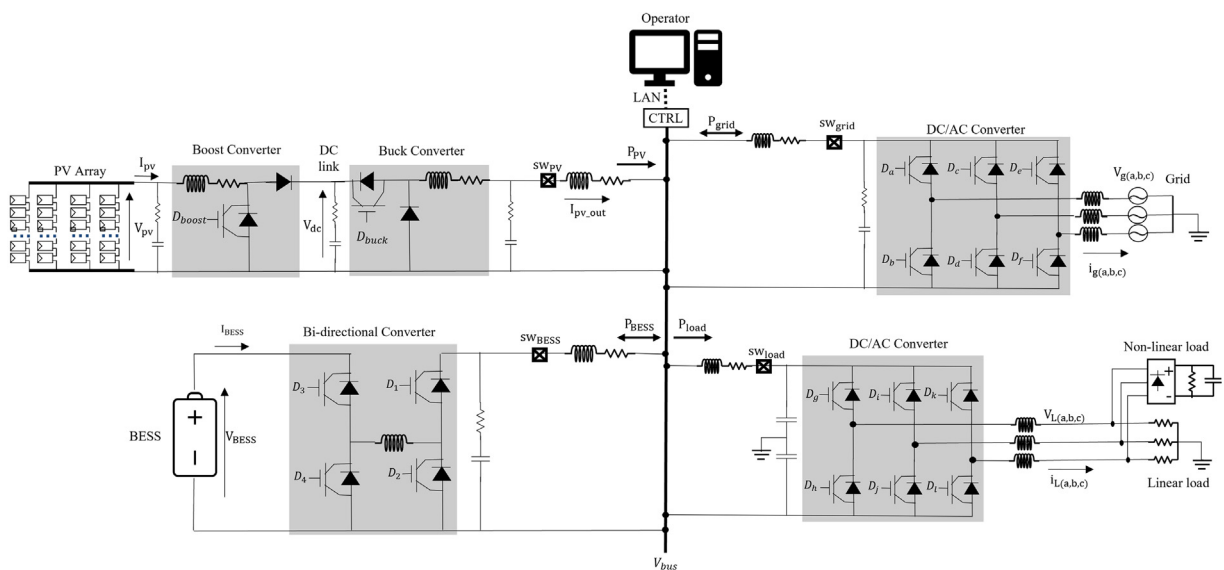

Fig. 1. System configuration: consists of the PV system, BESS, AC loads and a connection to the UG. Also connected is the power router module.

2.2. DC bus voltage control and power routing scheme

The converters in a DC MG can be categorized into two kind of terminals, namely power terminals and slack terminals [8]. Power terminals usually operate on their own merits by regulating the local power. They include source

power terminals (e.g., variable generations such as wind and photovoltaics which normally operate in MPPT) and load power terminals that supply or consume power respectively. On the other hand, slack terminals are controlled to maintain power balance and maintain the system voltage withing acceptable limits.

In the conventional voltage–power droop control shown in Fig. 2a, parallel slack converters are controlled to regulate the bus voltage to the same voltage Ref. [9]. DC voltage is a crucial index of power balance condition in a DC network. When there is excess source power, DC voltage increase while DC voltage decreases when the load power is greater than the source power. All parallel slack converters are regulated to absorb the excess power in proportion to their droop coefficient when there is an increase in bus voltage above the reference voltage while in the case where there is more load demand than the available source power, the converters discharge power in proportion to their droop coefficient. However, due to the presence of the droop coefficient and line resistance, there always exist a deviation of the bus voltage from the reference value. It is observed that in the conventional droop strategy, the power flow of all slack converters has the same direction (i.e., either they all absorb power or discharge power) in all operation condition.
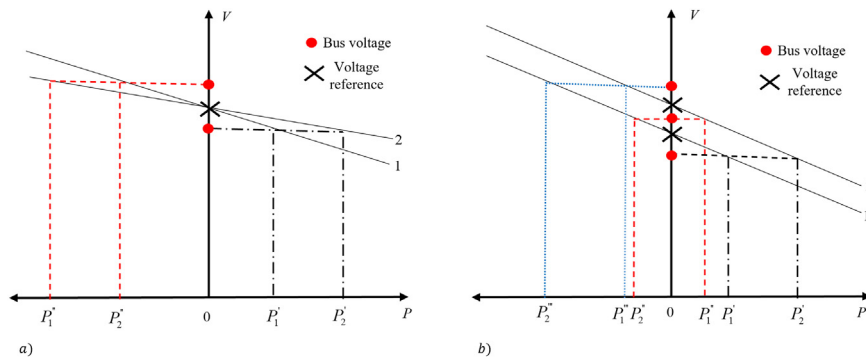

Fig. 2. Principle of (a) conventional droop control; (b) proposed control.

In the proposed strategy, the control of the bus voltage in the system is achieved by adopting different voltage reference values for the slack terminals as shown in Fig. 2b. Neglecting line resistances voltage drop, the bus voltage is the average of the slack terminals references. However, excess source power increases the bus voltage above the average value while excess load demand decreases the average bus voltage. Depending on the value of the bus voltage relative to the voltage references of the slack terminals, the desired power flow magnitude and direction within the slack terminals can be obtained.

In the studied MG, either or both the BESS and grid-VSC (G-VSC), when connected, acts as the slack to regulate the DC voltage in a range of 360–400 V with the PV operating in the MPPT mode. The voltage reference for the G-VSC is defined by the power router system whereas the voltage reference of the BESS is a function of its state of charge (SoC). A switching signal for the PV control is activated for mode change from MPPT to BVC when both the grid and the BESS are disconnected, and the load connected. Connection of the various terminals to the DC bus is done through controlled switches sw. A switch control signal of 0 signifies disconnected mode while 1 signifies connected mode. The power flow within the MG and exchange with the UG are based on the following principles:

(1) Peak load conditions: In case of periods with available PV power, priority is given to PV generation. When the PV power is inadequate, the BESS is discharged to supplement the excess requirement. In cases where the BESS does not meet the required load demand, purchase of power from the UG is considered. In cases where the BESS does not meet its discharge limit, sale of electricity to the UG is considered.

(2) Low load conditions: In case of abundant PV power, the BESS will be charged and sale of electricity to the grid is considered. In the island operation mode, and the BESS in full charge mode, the control of the PV is switched from MPPT to BVC mode.

In Fig. 3, a summary of some possible PR schemes is presented. A detailed description of the units and their control systems are given in the next section.
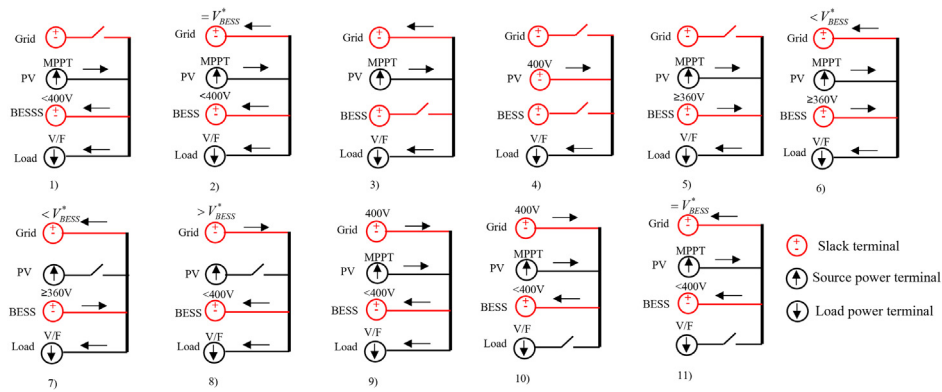
Fig. 3. Power routing and voltage control strategy for different operation modes.

3. Modelling of complete DC-microgrid system

3.1. PV system

The PV system consists of PV modules in series and parallel connections to form a PV array with total power of 13.445 kW at a voltage V_{mpp} of 422.8 V and current I_{mpp} of 31.8 A. Depending on the operating mode of the MG and environmental conditions such as temperature, irradiation conditions and shading effects, the PV voltage maybe higher or less than the bus voltage. Therefore, a DC converter with both a boost and buck functions is desirable to interface with the MG bus. The converter operates in two different control modes:

(a) MPPT mode: In this mode, the first stage boost converter is controlled by an MPPT controller (P&O method [10] is adopted) to track the maximum power from the PV array. The second stage buck converter controls the DC-link voltage to a constant value of 750 V and regulates the output current flowing into the grid. The duty ratio for the boost and buck converters in this mode are represented as D_{boost_mpp} and D_{buck_mpp} respectively. The MG bus voltage is controlled either by the G-VSC and/or the BESS converter.

(b) BVC mode: It represents the stand-alone operation of PV and load where the grid and battery are disconnected. In this mode, the boost converter is tasked to regulate the DC-link voltage to 750 V while the buck converter controls the MG bus voltage to 400 V. The duty ratio for the boost and buck converters in this mode are represented as D_{boost_vc} and D_{buck_vc} respectively.

The mode selection is based on the availability or absence of slack terminal in the network. A switching signal for the PV control is activated for mode change from MPPT to BVC when both the grid and the battery systems are disconnected. The controllers and mode selection algorithm are presented in Fig. 4a.

3.2. BESS

A lithium-ion BESS model with a total nominal battery capacity of 24 kWh and rated battery voltage of 360 V is adopted in the DC MG design. The battery model is connected to a four quadrant DC–DC buck-boost bidirectional converter. The converter operates as a four-quadrant chopper of voltage and current and can emulate standard buck and boost bidirectional converter circuits by operating different switches. The converter acts as a slack terminal in both charge and discharge modes of operation with the bus voltage reference defined by its SoC as shown in Table 1.

Table 1. BESS control.

SoC [%]	< 40	40–70	70–80	80–85	>= 85
V^*_{BESS}[V]	360	370	380	390	400

a) PV Control b) BESS Control c) Grid VSC Control d) Load Side VSI Control
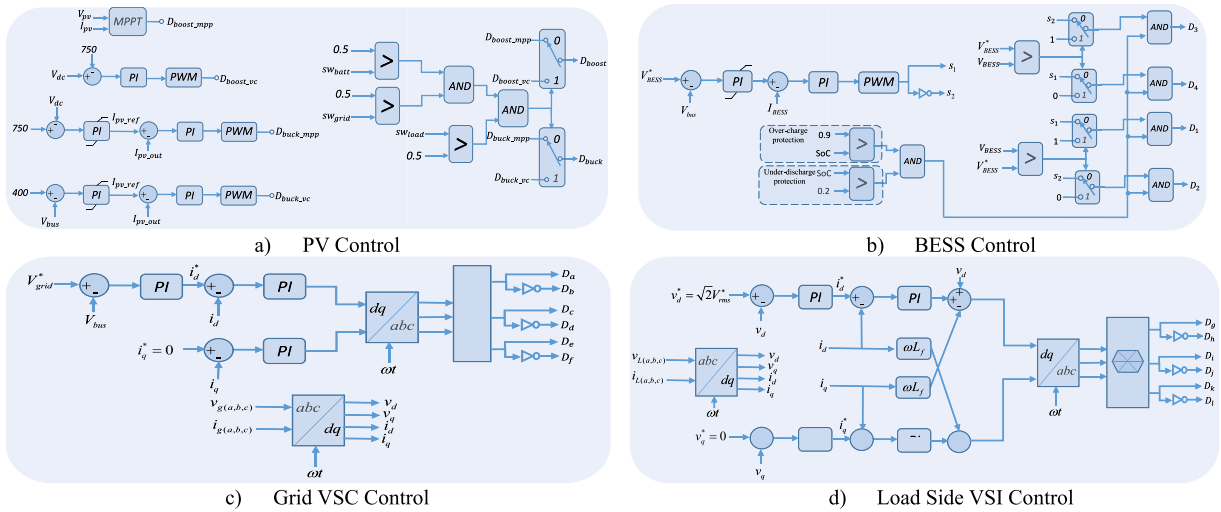
Fig. 4. Control diagrams of converters.

The schematic diagram of the battery system converter controller is depicted in Fig. 4b. During buck operation mode ($V_{BESS} < V_{BESS}^*$), the ON signal is always applied to D_3 and the OFF signal always applied to D_4. The pulse-width modulation (PWM) control is performed on D_1 and D_2. In the boost operation mode ($V_{BESS} > V_{BESS}^*$), the ON signal is always applied to D_1 and the OFF signal always applied to D_2. The PWM control is performed on D_3 and D_4. In both modes of operation, the direction of current flow will depend on the sign of the voltage error between the bus voltage and the reference value fed to the PI controller. Since the converter PWM switches are operated in a complementary way, it is sufficient to design a single control scheme that works in either the charge or discharge mode of operation. An inner current control loop regulates the discharge/charge current from/to the BESS. The controller also consists of an over-charge and under-discharge protection schemes. The battery circuit is disconnected when the SoC falls below 0.2 while in the discharging mode or above 0.9 while in the charging mode of operation.

3.3. Grid-voltage source converter control

The control method adopted for the G-VSC is the voltage-oriented control and it is depicted in Fig. 4c. The active current reference maintains the DC voltage to its reference value defined by the power router configuration. The reference value ranges from 360–400 V in steps of 10 V. The reactive current reference is set to 0 to maintain a unity power factor.

3.4. Loads

The loads are modelled as both linear and non-linear loads. The non-linear load is modelled as a three-phase uncontrolled diode bridge rectifier with a DC capacitor supplying a resistive load. The voltage source inverter (VSI) controls the frequency and voltage at the load side using the space vector modulation technique. The root-mean-squared value of the output phase voltage and frequency are 200 V and 60 Hz respectively. The VSI controller is depicted in Fig. 4d. For resistive loads, the d-axis reference voltage is expressed as: $v_d^* = \sqrt{2}V_{rms}^*$, where V_{rms}^* is the output RMS phase voltage reference value.

4. Simulation studies

In other to validate the proposed control methods, simulation tests have been carried out in terms of steady state performance and transient performance between the modes presented in Fig. 3. It should be noted that, the proposed

method can support all possible combination of mode transitions. The power flow from all terminals and bus voltage are shown in the results.

Fig. 5a represents the transition process from Mode 1 to Mode 2. The PV operating in MPPT mode supplies power to both the BESS and the loads. The bus voltage is regulated by the BESS to 360 V. However, excess PV power increases the bus voltage to 378 V. At 150 ms, the grid is connected with voltage reference less than the bus voltage. In this way, power flow is from the PV to all the three terminals. The bus voltage is regulated by both BESS and G-VSC to around 363 V.
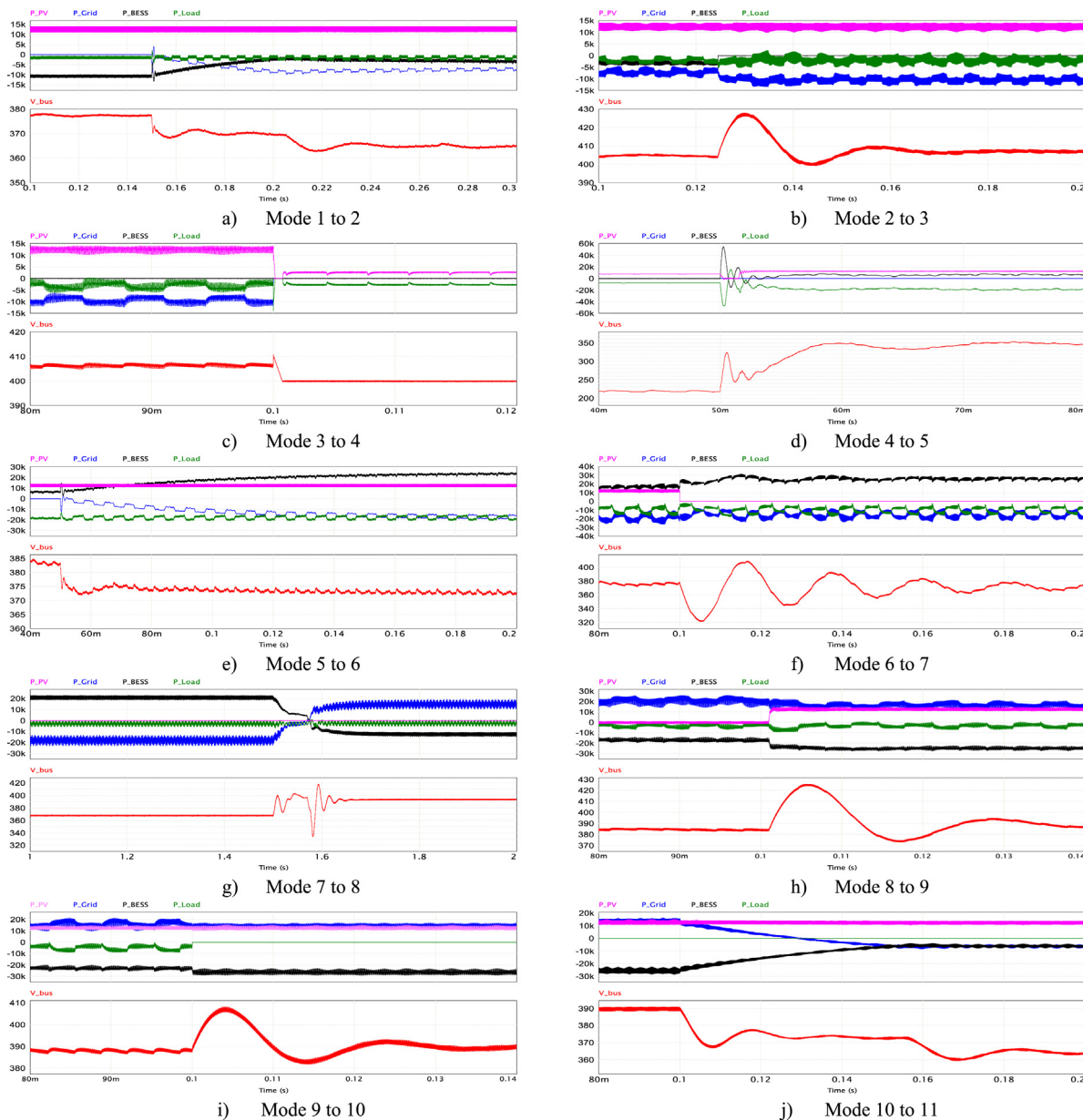

Fig. 5. Steady state operation and transition process between Modes. For the power curves; colour 'pink' indicates PV power, 'blue' indicates grid power, 'black' indicates BESS power and 'green' indicates Load power. The MG bus voltage is indicated in colour 'red' below the power curves. (For interpretation of the references to colour in this figure legend, the reader is referred to the web version of this article.)

Fig. 5b represents the transition from Mode 2 to Mode 3. At about 125 ms, the BESS is disconnected at full charge. The power flow to the grid from the PV is increased with a minor increase in bus voltage magnitude.

Fig. 5c represents the transition from Mode 3 to Mode 4. At about 100 ms, sale of power from the MG to the UG is interrupted by disconnection of the G-VSC. With no slack terminal in the system, the PV control switches from MPPT to BVC mode. The PV reduces its power to match the low load power. This bus voltage is regulated to 400 V.

Fig. 5d represents the transition from Mode 4 to Mode 5. In mode 4, the PV output is inadequate to match the load demand. This results in bus voltage around 220 V. The BESS is connected at 50 ms to supply the additional load demand. Bus voltage control is taken over by the BESS. High transient power is because of the lack of protection scheme.

Fig. 5e represents the transition from Mode 5 to Mode 6. The G-VSC is connected at 50 ms with reference voltage less than the BESS and bus voltage to operate in power absorption mode. The BESS increases its output power to match the power demand.

Fig. 5f represents the transition from Mode 6 to Mode 7. The PV is disconnected at 100 ms because of no sun light. The BESS increases its output to match the load demand and export to the grid.

Fig. 5g represents the transition from Mode 7 to Mode 8. With the PV still disconnected, the flow of power between the grid and BESS is reversed at 150 ms. Power is imported from the grid to meet the load demand and charge the BESS. The bus voltage undergoes a short transient and settles at a new steady state.

Fig. 5h represents the transition from Mode 8 to Mode 9. The PV is connected at 100 ms. The PV has a short delay in reaching its maximum power. The charging power of the BESS increases accordingly with a minor reduction in power import from the grid.

Fig. 5i represents the transition from Mode 9 to Mode 10. At 100 ms, the load is disconnected. The excess power from the PV and the grid is absorbed by the BESS in the charging mode.

Fig. 5j represents the transition from Mode 10 to Mode 11. At 100 ms, the G-VSC reference is reduced to same value as BESS reference. In this way, the PV power charges the BESS and also exported to the grid. The bus voltage settles in a new steady state value.

5. Conclusion

In this paper, a robust DC microgrid operation for power exchange between the microgrid and the utility grid has been proposed. When connected, both the BESS and utility grid terminals are operated in the slack mode at the same or different terminal voltages to enable intentional power routing. In this way, both the direction and magnitude of power flow can be controlled with the voltage setpoints. Control methods for PV, BESS, load and utility grid converters have been developed. The feasibility of the proposed scheme has been validated by simulation results performed in PSIM environment. Simulation tests have been carried out in terms of steady state performance and transient performance between different operation modes. The power flow from all terminals and bus voltage are shown in the results.

Declaration of competing interest

The authors declare that they have no known competing financial interests or personal relationships that could have appeared to influence the work reported in this paper.

References

[1] Dragicevic T, Guerrero JM, Vasquez JC, Skrlec D. Supervisory control of an adaptive-droop regulated DC microgrid with battery management capability. IEEE Trans Power Electron 2014;29(2):695–706.

[2] dos Santos Neto PJ, Barros TAS, Silveira JPC, Ruppert Filho E, Vasquez JC, Guerrero JM. Power management techniques for grid-connected DC microgrids: A comparative evaluation. Appl Energy 2020;269(25920):115057.

[3] Ding T, Lin Y, Bie Z, Chen C. A resilient microgrid formation strategy for load restoration considering master–slave distributed generators and topology reconfiguration. Appl Energy 2017;199:205–16.

[4] Xiao J, Wang P, Setyawan L. Implementation of multiple-slack-terminal DC microgrids for smooth transitions between grid-tied and islanded states. IEEE Trans Smart Grid 2016;7(1):273–81.

[5] Kumar J, Agarwal A, Agarwal V. A review on overall control of DC microgrids. J Energy Storage 2019;21(2018):113–38.

[6] Al-ismail FS, Member S. DC microgrid planning, operation, and control: A comprehensive review. IEEE Access 2021;9.

[7] Lu X, Guerrero JM, Sun K, Vasquez JC, Teodorescu R, Huang L. Hierarchical control of parallel AC–DC converter interfaces for hybrid microgrids. IEEE Trans Smart Grid 2014;5(2):683–92.

[8] Chen D, Xu L. Autonomous DC voltage control of a DC microgrid with multiple slack terminals. IEEE Trans Power Syst 2012;27(4):1897–905.

[9] Shuai Z, Fang J, Ning F, Shen ZJ. Hierarchical structure and bus voltage control of DC microgrid. Renew Sustain Energy Rev 2018;82(2):3670–82.

[10] Alik R, Jusoh A. An enhanced P & O checking algorithm MPPT for high tracking efficiency of partially shaded PV module. Sol Energy 2018;163:570–80.